COMMUNICATIONS

Multiple liquid–liquid transitions in supercooled water

Ivan Brovchenko, Alfons Geiger, and Alla Oleinikova
Physikalische Chemie, Universität Dortmund, D-44221 Dortmund, Germany

(Received 17 January 2003; accepted 31 March 2003)

Three distinct liquid–liquid coexistence regions were observed for ST2 model water by restricted ensemble Monte Carlo simulations of the isotherms of homogenized systems and by phase equilibria simulations in the Gibbs ensemble. The lowest density liquid–liquid transition meets the liquid–vapor phase transition at a triple point and ends in a metastable critical point. A percolation analysis evidences, that the phase separations at the lowest and highest densities can be attributed to the separation of differently coordinated water molecules. The densities of the obtained four phases of supercooled water correlate with experimentally observed densities of amorphous ice. © *2003 American Institute of Physics.* [DOI: 10.1063/1.1576372]

The anomalies of liquid water at ambient and low temperatures may be attributed to the existence of a liquid–liquid phase transition in the supercooled region. This hypothesis is based on the experimental observation of a first-order-like phase transition between low-density and high-density amorphous ices.[1] Additionally, computer simulations with different interaction models evidence a liquid–liquid transition in supercooled water (ST2,[2] TIP5P,[3] TIP4P[4]), indicated by sharp density changes in the isotherms (isobars). The position and density interval of the two-phase region varies essentially in these studies. This may be caused both by the differences in the water models and by shortcomings of the applied methods. In particular, it is difficult to control the metastability of the simulated state and phase separation in the simulation box, performing simulations in NVT or NPT ensembles. This prevents an accurate location of the liquid–liquid phase transition, especially the evaluation of the coexisting densities, and may cause an underestimation of the critical temperature. Moreover, additional liquid-liquid phase transitions may be missed, and therefore, the phase transitions reported in Refs. 2–4 may be of different nature.

The goal of our study is to investigate by use of a broadly examined water model and by appropriate and independent simulation methods the existence of liquid–liquid equilibria in supercooled water in a wide density range, in order to clarify their number and their location with respect to the liquid–vapor coexistence curve. Recently, the possibility of multiple liquid–liquid phase transitions in the melts of polymorphic solids-like ice was discussed.[5,6]

In this Communication we report coexistence between different states of supercooled water, observed by restricted ensemble simulations of the isotherms of homogeneous systems[7,8] and by simulations in the Gibbs ensemble.[9] Systems of 500 to 1000 ST2 water molecules[10] were simulated by the corresponding Monte Carlo (MC) methods with a simple spherical cutoff of the intermolecular interactions at 9 A and long-range corrections for the Lennard-Jones interactions (more details will be given in a forthcoming paper, Ref. 11). Thus we use the ST2 model as originally derived by Stillinger and Rahman,[10] without reaction field, as it has been used in later simulations. This model (including the cutoff) has been parametrized to reproduce the equilibrium densities of liquid water and its temperature maximum very closely (this will be discussed with Fig. 2), whereas subsequent additions to the model lead to a deviating behavior of this model liquid (see triangles in Fig. 2, for detailed investigations of the influence of the reaction field see Ref. 12).

The full liquid–vapor coexistence curve of this ST2 water model, obtained by Gibbs ensemble Monte Carlo (GEMC) simulations, is shown in Fig. 1. Each pair of equilibrium states is the result of an extensive simulation run of about 10^5 steps. Each step consists of up to 10^5 attempts to transfer a molecule between the two simulation boxes, 2 attempts to change their volumes and 10^3 translational and rotational molecular moves. The number of successful molecular transfers in each simulation run ranged from 10 to 100 per molecule. The critical temperature $T_C = 550.2$ K and critical density $\rho_C = 0.286$ g/cm^3 were obtained from a fit of the order parameter and diameter to a scaling law. A step–like change of the liquid density is observed at $T = 270$ K. Only at this temperature the liquid density depends on the initial configuration and therefore two points are shown in Fig. 1 (this is clearly not the case for $T = 265$ or $T = 275$ K). This finding indicates the possibility of a triple point, where the vapor phase and two liquid phases coexist. A similar temperature dependence of the density with a step–like course has been observed for a silicon melt, which also belongs to the class of tetrahedrally ordered liquids.[13]

Isotherms of ST2 water were obtained by simulations in a restricted NPT ensemble. The cubic simulation box with 513 molecules was divided into 27 equal cubic subcells which contain an equal number (19) of molecules. Typically from $1*10^5$ to $2*10^5$ translational and rotational molecular moves per molecule were done in the course of a MC simulation run. The number of molecules in the subcells was kept unchanged in the course of the simulations by rejecting MC

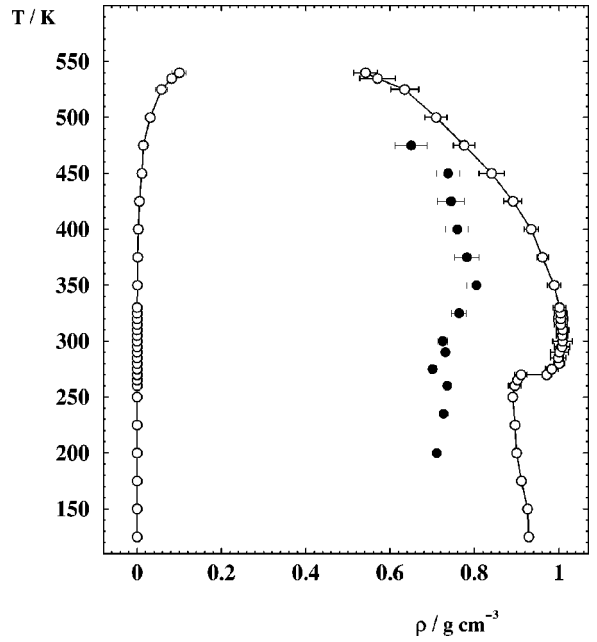

FIG. 1. Liquid–vapor coexistence curve of ST2 water, obtained by GEMC simulations (open circles, the line is a guide for the eyes only); liquid spinodal, obtained by simulations in the restricted NPT ensemble (closed circles).

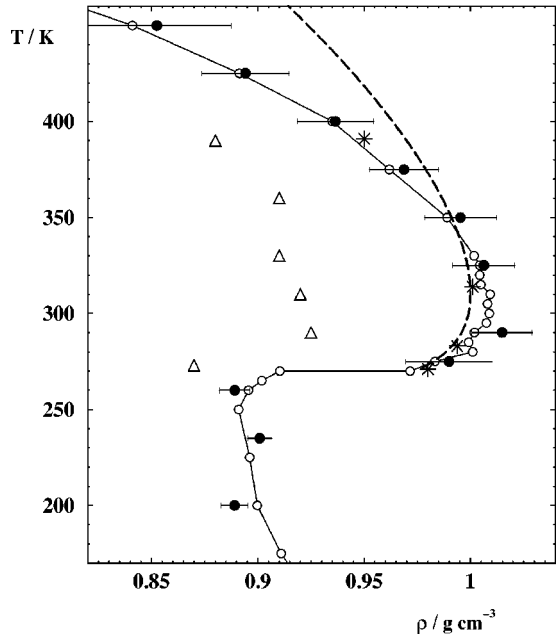

FIG. 2. Part of the liquid branch of the liquid–vapor coexistence curve of ST2 water. Open circles—GEMC simulation. Solid circles—isobar, simulated in the restricted NPT ensemble at $P=0$. Stars—$P=0$ isobar from Ref. 10. Dashed line—experimental data,[14] shifted up by 33 K. Triangles—$P=0$ isobar, interpolated from the data of Ref. 2.

moves, which violate the imposed constraint. Similar to restricted NVT ensemble simulations,[7,8] the constraints prevent a possible phase separation in the simulation box and allow a controlled extension of the isotherms into the metastable region. The difference is, that in the restricted NPT ensemble for a given pressure we have to start at different initial densities to locate both stable and metastable states on a given isotherm. The formation of unstable states is practically impossible in the NPT ensemble (the system moves to the next stable or metastable state by adjusting its volume). In order to test possible effects of constraints on the thermodynamical properties of water we simulated the $P=0$ isobar in the restricted NPT ensemble and compared it with the results of the GEMC simulation of the liquid–vapor coexistence curve (Fig. 2). There are no differences within the accuracy of the simulations.

An estimate of the liquid spinodal of the liquid–vapor transition is shown in Fig. 1. The closed circles indicate the lowest in a sequence of simulation runs with decreasing pressures, where water remained in a metastable liquid state and did not evaporate (which shows up as a strong expansion of the simulation box). When the temperature decreases, the pressure along the spinodal monotonically decreases and achieves roughly -5.3 kbar at $T=200$ K.

The computed low–temperature ST2-water isotherms are given in Fig. 3. Three liquid–liquid phase transitions are clearly seen at $T=235$ K. With increasing temperature the third phase transition disappears at $T\approx 260$ K, the second phase transition disappears at $T\approx 275$ K and the first phase transition disappears at $T\approx 290$ K. In view of the absence of the unstable region of the simulated isotherms, we estimate the location of the phase transition as the center of the pressure interval, where two phases are observed. In Fig. 4 the estimated densities (full symbols) of the three liquid–liquid coexistence curves are shown together with the liquid branch of the liquid–vapor coexistence curve. The lowest density liquid–liquid phase transition enters the liquid–vapor coexistence at the assumed triple point at $T=270$ K and ends at a critical point located at negative pressure in the region, where the liquid is metastable with respect to evaporation.

The reliability of the obtained results was checked by additional GEMC simulations of the liquid–liquid coexistence. Due to the extremely low acceptance probability of molecular transfers between two dense liquid phases at low temperatures these simulations were restricted to temperatures above 260 K and densities below 1.3 g/cm^3. In addition, the small density difference between the coexisting phases complicates the choice of the average total density in the two simulation boxes. Therefore, GEMC simulation runs were started at many different values of the total density. Each run was treated as in the liquid–vapor coexistence case, but here we achieved only 1 to 2 transfers per molecule, even in simulations runs, which took several months of computer time on a GHz processor. This was sufficient to reach the same equilibrium, when starting from different initial densities. Phase separation was observed in the GEMC simulations very close to the location of the first and second liquid–liquid phase transitions, which had been obtained from the isotherms of the restricted ensemble simulations (see Fig. 4). Both transitions disappear at $T=280$ K. Note also, that additional GEMC simulations at different state points confirmed the absence of further phase transitions in the investigated range of density and temperature.

The location of the obtained liquid–liquid phase transitions in the pressure-temperature plane is shown in Fig. 5. The first liquid–liquid transition crosses the liquid–vapor phase transition ($P\approx 0$) at about $T=270$ K, which coincides

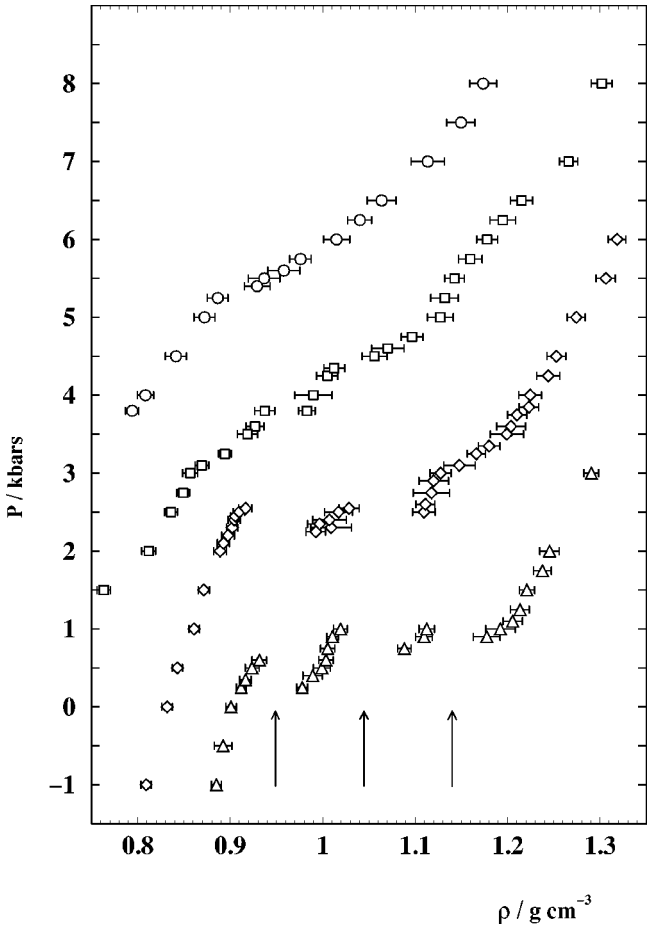

FIG. 3. Isotherms of ST2 water, obtained in restricted NPT ensemble simulations. $T=290$ K (circles), $T=275$ K (squares), $T=260$ K (diamonds), $T=235$ K (triangles). The given pressures hold for the 235 K isotherm. The subsequent isotherms are shifted by 2, 4, and 6 kbar, respectively. Three liquid–liquid phase transitions are indicated by arrows.

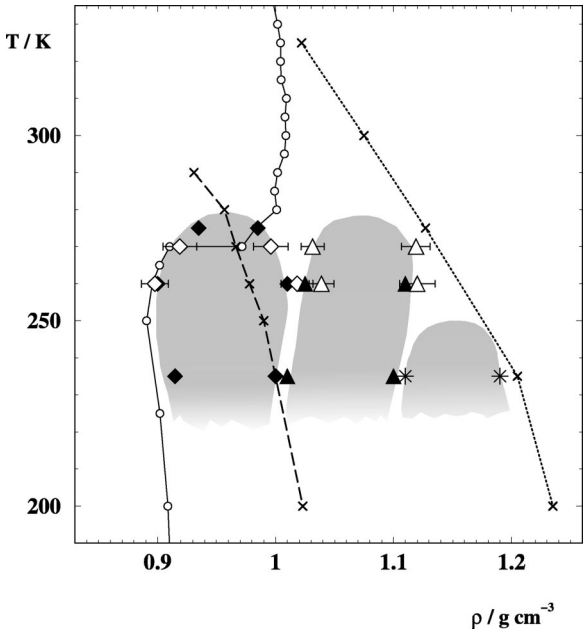

FIG. 4. Liquid–liquid and liquid–vapor coexistence regions of ST2 water. Open symbols—from GEMC simulation. Closed symbols—from restricted NPT ensemble simulations. Circles—see caption of Fig. 1. Diamonds—first liquid–liquid transition. Triangles—second liquid–liquid transition. Stars—third liquid-liquid transition. Dotted and dashed lines—percolation thresholds of tetrahedral and perfectly tetrahedral water molecules, respectively (see text). Shadowed areas show a rough estimate of the liquid–liquid two-phase regions.

with the sharp decrease of the liquid density at the same temperature (Fig. 1). It ends in a metastable critical point, which is located at $T\approx 280$ K and $P\approx -300$ to -500 bar. The liquid spinodal of this transition, estimated from the corresponding isotherms (Fig. 3), crosses the line of the liquid–vapor transition ($P\approx 0$ bar) a few degrees below 270 K. This means, that the liquid phase in equilibrium with its vapor approaches a singularity with decreasing temperature, giving an explanation for the experimentally observed apparent singular behavior of supercooled water.[15] The interval between the temperature of maximum density and the singular temperature at zero pressure, for our model ST2 water is about 40 K in comparison with the experimental value of 49 K, obtained from the measurements of the compressibility of water.[15] The overall shift of the simulated results to higher temperatures by about 30–35 K, if compared with experimental data, is in agreement with the previous simulations.[2,10]

The separation of a one–component system into two liquid phases is usually attributed to the existence of molecules with different local ordering. To identify the different molecular species, which may be responsible for the phase separation, we applied a percolation analysis. Recently, we found in an aqueous solution that the liquid–liquid binodal (spinodal) is close to the percolation thresholds of the components.[16] The natural choice of a distinct ''component'' in pure water are ''tetrahedrally ordered'' water molecules. These are defined by the tetrahedricity measure,[17,18] which describes the deviation of the tetrahedra formed by the four closest neighbors from the perfect equilateral geometry.

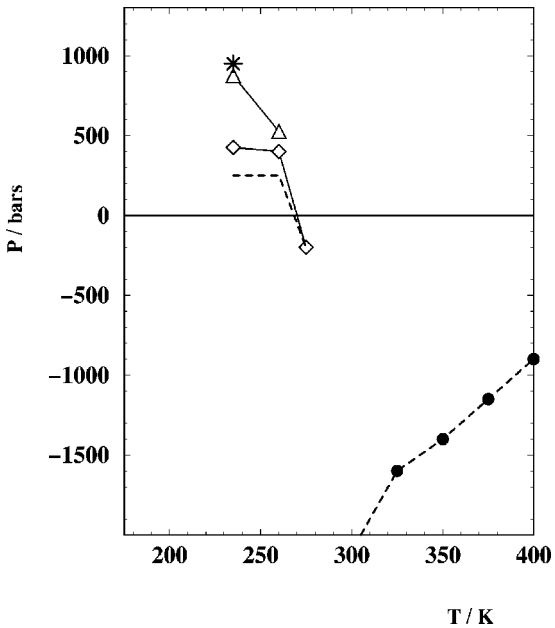

FIG. 5. Phase diagram of supercooled ST2 water. Diamonds and dashed line—first liquid–liquid transition and one of its spinodals. Triangles and star—second and third liquid–liquid phase transition. Full circles—liquid spinodal of the liquid–vapor transition.

The line of percolation thresholds of these molecules (Fig. 4, dotted line) was obtained from conventional MC simulations in the NVT ensemble at various densities with about $1*10^5$ to $2*10^5$ molecular displacements and rotations per molecule. It represents the high-density boundary for the obtained regions of liquid–liquid immiscibility. To the right of this line the fraction of the tetrahedral molecules is not high enough to establish percolation of this species. If we define as a distinct component ''perfectly coordinated tetrahedral molecules,'' which have—in addition to the demanded tetrahedricity measure—exactly four nearest neighbors in the first coordination shell, the percolation threshold is found close to the binodal (spinodal) of the first liquid–liquid phase transition (dashed line in Fig. 4). This finding shows that this transition is caused by the separation of the perfect tetrahedral molecules in agreement with the results of Ref. 2, where the low density water phase consists of water molecules with four neighbors in the first coordination shell. To elucidate the nature of the other observed liquid–liquid transitions, the local ordering of water molecules should be analyzed in more details, probably based on the structures of high density ices.

Only one liquid–liquid phase transition with a critical point at positive pressures and below 250 K was found in Ref. 2 for the ''same'' ST2 water model. The reason for the disagreement with our results is the treatment of the long-range interactions which means in principle the use of different interaction models, as indicated above. (First results of extended simulations with the ST2 water model including the reaction field and using both GEMC and restricted NPT ensembles,[11] agree with the data of Ref. 2.) The use of the reaction field method for the long–range Coulombic interaction apparently strengthens the water hydrogen bonding and as a result shifts the liquid density at $P=0$ towards lower values compared to both experimental[14] and the original ST2 model data[10] (see Fig. 2). As a result, the low density liquid–liquid transition shifts to lower temperatures and positive pressures and therefore may be separated from the liquid–vapor transition, thus opening a continuous path to the lowest density water.[18] Such a shift of the phase diagram with strengthening hydrogen bonds agrees with the predictions of the modified van der Waals model for water.[19]

For the TIP4P water model, which exhibits essentially weaker tetrahedral ordering, we performed similar simulations and observe two liquid–liquid phase transitions.[11] The critical temperatures of both transitions are located between 175 and 200 K, whereas the critical pressure is about -1.0 kbar and $+1.0$ kbar for the first and the second transition, respectively. Contrary to the ST2 water model, the first transition of the TIP4P water model does not show a triple point with the liquid–vapor transition (at least at $T>100$ K).

From this study we conclude, that real water may develop a multiplicity of liquid–liquid phase transitions with a first liquid–liquid critical point at negative pressures (in agreement with the proposition, made in Ref. 4). The expectation of multiple liquid–liquid transitions is in accord with the recent observation of several metastable states of amorphous ice.[20] Note that the densities of the four phases of supercooled water, obtained in our simulation (see the $T=235$ K isotherm of Fig. 3), correlate with the available experimental data on the densities of amorphous forms of water at $T=77$ K and $P=0$: low-density amorphous ice[1] ($\rho=0.94$ g/cm^3); hyperquenched amorphous water[21] ($\rho=1.04$ g/cm^3); high-density amorphous ice[1,22] ($\rho=1.17-1.19$ g/cm^3, $\rho=1.14-1.15$ g/cm^3); very-high-density amorphous ice[22] ($\rho=1.25-1.26$ g/cm^3). Finally, it should be mentioned, that two liquid–liquid phase transitions were also observed for a waterlike model fluid confined between hydrophobic surfaces.[23]

ACKNOWLEDGMENTS

This work was supported by the Ministerium fur Wissenschaft und Forschung des Landes Nordrhein-Westfalen and by DFG Forschergruppe 436.

[1] O. Mishima, L. D. Calvert, and E. Whalley, Nature (London) **314**, 76 (1985); O. Mishima, Phys. Rev. Lett. **85**, 334 (2000).
[2] P. H. Poole, F. Sciortino, U. Essmann, and H. E. Stanley, Nature (London) **360**, 324 (1992); F. Sciortino, P. H. Poole, U. Essmann, and H. E. Stanley, Phys. Rev. E **55**, 727 (1997); S. Harrington, R. Zhang, P. H. Poole, F. Sciortino, and H. E. Stanley, Phys. Rev. Lett. **78**, 2409 (1997).
[3] M. Yamada, S. Mossa, H. E. Stanley, and F. Sciortino, Phys. Rev. Lett. **88**, 195701 (2002).
[4] H. Tanaka, Nature (London) **380**, 328 (1996); J. Chem. Phys. **105**, 5099 (1996).
[5] V. V. Brazshkin, R. N. Voloshin, A. G. Lyapin, and S. V. Popova, Physics-Uspekhi **42**, 941 (1999).
[6] H. Tanaka, Phys. Rev. E **62**, 6968 (2000).
[7] J.-P. Hansen and L. Verlet, Phys. Rev. **184**, 151 (1969).
[8] D. S. Corti and P. G. Debenedetti, Chem. Eng. Sci. **49**, 2712 (1994).
[9] A. Z. Panagiotopoulos, Mol. Phys. **62**, 701 (1987).
[10] F. H. Stillinger and A. Rahman, J. Chem. Phys. **60**, 1545 (1974).
[11] I. Brovchenko, A. Geiger, and A. Oleinikova (unpublished).
[12] P. E. Smith and W. F. van Gunsteren, Mol. Simul. **15**, 233 (1995); D. van der Spoel, P. J. van Maaren, and J. C. Berendsen, J. Chem. Phys. **108**, 10220 (1998).
[13] C. A. Angell, S. Borick, and M. Grabow, J. Non-Cryst. Solids **205–207**, 463 (1996).
[14] W. Wagner and A. Prus, J. Phys. Chem. Ref. Data **31**, 387 (2002) (above 273 K); D. E. Hare and C. M. Sorensen, J. Chem. Phys. **87**, 4840 (1987) (below 273 K).
[15] H. Kanno and C. A. Angell, J. Chem. Phys. **70**, 4008 (1979).
[16] A. Oleinikova, I. Brovchenko, A. Geiger, and B. Guillot, J. Chem. Phys. **117**, 3296 (2002).
[17] N. N. Medvedev and Y. I. Naberukhin, J. Non-Cryst. Solids **94**, 402 (1987).
[18] D. Paschek and A. Geiger, J. Phys. Chem. B **103**, 4139 (1999).
[19] P. H. Poole, F. Sciortino, T. Grande, H. E. Stanley, and C. A. Angell, Phys. Rev. Lett. **73**, 1632 (1994).
[20] C. A. Tulk, C. J. Benmore, J. Urquidi, D. D. Klug, J. Neuefeind, B. Tomberli, and P. A. Egelstaff, Science (Washington, DC, U.S.) **297**, 1320 (2002).
[21] W. E. Brower, Jr., D. J. Schedgick, and L. K. Bigelow, J. Phys. Chem. B **106**, 4565 (2002).
[22] T. Loerting, C. Salzmann, I. Kohl, E. Mayer, and A. Hallbrucker, Phys. Chem. Chem. Phys. **3**, 5355 (2001).
[23] T. M. Truskett, P. G. Debenedetti, and S. Torquato, J. Chem. Phys. **114**, 2401 (2001).